Modeling Urban Storm-Water Quality Treatment: Model Development and Application to a Surface Sand Filter

Pedro Avellaneda[1]; Thomas Ballestero, Ph.D., P.E.[2]; Robert Roseen, Ph.D., P.E.[3]; and James Houle[4]

Abstract: A mathematical and statistical model for simulating contaminant removal from a surface sand filter is reported. The model was based on a mass balance equation and an advection-dispersion transport model. The unknown parameters of the model were the deposition rate and the hydrodynamic dispersion. Changes in space were allowed within the filter media depth and time variability of flow and influent contaminant concentration were taken into account. System field monitoring was performed between 2004 and 2006. A total of 17 storms were selected for the study. Runoff constituent analyses included: total suspended solids, total petroleum hydrocarbons-diesel range hydrocarbons, and zinc. The objective was to explore the capabilities of a two parameter model for predicting effluent contaminant concentrations. Optimized model parameter values were calculated on a storm by storm basis. Thereafter, a gamma distribution was fitted to the optimized values. A Monte Carlo simulation was performed to explore the predicting capabilities of the model by using two storms left for validation. Results of the validation phase show an acceptable performance of the model since, in general, estimated effluent concentrations fell within the uncertainty limits.

DOI: 10.1061/(ASCE)EE.1943-7870.0000124

CE Database subject headings: Stormwater management; Urban areas; Hydraulic models; Sand, filter; Parameters; Estimation; Water treatment.

Author keywords: Stormwater modeling; Sand filtration; Parameter estimation.

Introduction

Our awareness of storm water impacts has led us to the development of different storm-water treatment strategies. Previous knowledge regarding traditional water treatment systems (drinking and wastewater) and the evaluation of current storm-water treatment strategies has helped designers understand what is appropriate to mitigate the deleterious effects of storm water. The final selection of a site specific storm-water treatment system is driven by: the quantity of water to treat; contaminants to remove; peak flow; treatment efficiency; regulatory constraints; cost; and other design factors (Minton 2002). During the last decade, storm water has been considered the next environmental challenge to be addressed (EPA 1996).

The surface sand filter is one of the storm-water treatment measures recommended for storm-water mitigation, yet not commonly selected. The system appears in state storm-water design manuals and its performance has been documented (EPA 1999; Keblin et al. 1998; Minton 2002; Roseen et al. 2006). Design criteria for sand filters are based on the hydraulic capacity and removal characteristics of the filter media (Urbonas 1999). It has been shown that sand filters are able to achieve high removal efficiencies for sediments and biochemical oxygen demand when the system is properly maintained. Total metal removal is moderate and nutrient removal is often low. Water quality performance of the sand filter can be evaluated by comparing influent and effluent event mean concentrations (EMCs). The EMC of a storm event is defined as the total contaminant load (influent or effluent) divided by the total water volume. Barrett (2003) concluded, based on a regression analysis of influent and effluent EMCs, that the effluent concentration of sediment and particle-associated constituents is generally independent of the influent concentration.

Although the sand filter's performance has been reported in numerous studies, there is little research investigating the usage of mathematical and statistical models to describe the time variation of the effluent concentrations from a surface sand filter. If the water quality attributes of the sand filter can be confidently modeled then managers, regulators, engineers, and scientists will be provided with tools for planning and management. Moreover, efforts are needed to undertake the problem of predicting effluent concentrations.

Iwasaki (1937) proposed a filtration theory that describes a decrease in concentration within the filter depth as function of the input concentration and a filtration coefficient. The removed suspended particles accumulate in the filter pores. Iwasaki's model also provides a mathematical expression for determining the accumulation of suspended particles within the filter media. Time

[1]Graduate Research Assistant, Water Resources, Dept. of Civil Engineering, Univ. of New Hampshire, 230 Gregg Hall, 35 Colovos Rd., Durham, NH 03824 (corresponding author). E-mail: pmavellaneda@gmail.com

[2]Associate Professor, Civil Engineering, Dept. of Civil Engineering, Univ. of New Hampshire, 35 Colovos Rd., Durham, NH 03824. E-mail: tom.ballestero@unh.edu

[3]Assistant Research Professor, Civil Engineering, Dept. of Civil Engineering, 35 Colovos Rd., Univ. of New Hampshire, Durham, NH 03824. E-mail: robert.roseen@unh.edu

[4]Outreach Coordinator, Program Manager, The UNH Stormwater Center, 35 Colovos Rd., Univ. of New Hampshire, Durham, NH 03824. E-mail: james.houle@unh.edu

Note. This manuscript was submitted on April 28, 2008; approved on June 29, 2009; published online on July 17, 2009. Discussion period open until June 1, 2010; separate discussions must be submitted for individual papers. This paper is part of the ***Journal of Environmental Engineering***, Vol. 136, No. 1, January 1, 2010. ©ASCE, ISSN 0733-9372/2010/1-68–77/$25.00.

variability of the filtration coefficient is expected due to the accumulation of suspended particles. Iwasaki's model has been used in combination with other physicochemical and biological models to simulate slow sand filtration in drinking water and porous media applications (Campos et al. 2006a,b; Mayes and Hunt 2005; Li and Davis 2008a,b; Boyd and Ghosh 1974). However, the model is developed for constant flow and influent concentration. One challenge with storm-water modeling is the inherent time variability of variables such as: influent flows, influent concentrations, particle size, and temperature.

Transport processes can be described by advection-dispersion models. The transport equation for filtration applications incorporates a deposition rate coefficient that accounts for the accumulation of particulate matter (Kretzschmar et al. 1997). Other studies (Yao et al. 1971; Tufenkji and Elimelech 2004) have shown the relationship between the deposition rate coefficient and other parameters such as: porosity, grain diameter, filter depth, average travel time of a particle, and factors related to the efficiency of the filter media.

The objectives of this study were: (1) to develop a model for estimating effluent contaminant concentrations from a surface sand filter incorporating an advection-dispersion model; (2) to provide optimized parameters on a storm by storm basis and identify a probability distribution to describe its variability; and (3) to perform a Monte Carlo simulation to explore the capabilities of the model for estimating effluent contaminant concentrations. The parameters of the model were the hydrodynamic dispersion and deposition rate coefficients. The surface sand filter was monitored for storm-water quality at a parking lot in Durham, N.H. System field monitoring was performed between 2004 and 2006. A total of 17 storms were selected for the study. Runoff constituent analyses included: total suspended solids (TSS), total petroleum hydrocarbons-diesel range hydrocarbons (TPH-D), and zinc (Zn).

The organization of this paper is as follows. First, a description of the surface sand filter and the monitoring program is presented. Second, a description of the statistical and mathematical model is provided along with the numerical techniques for the solution of the transport equation and optimization. Lastly, results of the calibration and validation phase are reported for selected runoff events.

Surface Sand Filter

The surface sand filter monitored for this research is located at the University of New Hampshire Stormwater Center in Durham. A commuter parking lot provides the storm-water runoff to the filter. The treatment system is a design comprised of a sedimentation forebay and filter basin. The forebay bottom is 2.4×3.2 m ($A_f=7.68$ m^2) and the filter bed is 2.4×6.1 m ($A_{sf}=14.6$ m^2). The filter is 0.76 m high and uses coarse to medium grain sand with $d_{10}=0.3$ mm, $d_{50}=0.7$ mm, and $d_{85}=2$ mm. The sedimentation forebay helps remove the largest particles and allows for flow equalization. The forebay was designed to hold 25% of the water quality volume (WQV) (25 mm of precipitation on 4,047 m^2 of watershed). The designed WQV was 92.5 m^3 and corresponds to the daily storm volume not exceeded 90% of the days with measurable precipitation. The sedimentation forebay and the basin above the filter media are connected by a 0.15-m diameter pipe with a 25-mm orifice plate. The basin above the sand filter media can hold the remaining 75% WQV. Temporary ponding is expected during larger storm events due to saturation of the filter media and the fact that inflow exceeds outflow. The filter bed is subdrained by a 0.15-m diameter perforated pipe bedded in a 0.20-m layer of crushed stone ($d_{50}=19$ mm). Design parameters were adopted from the *New York State Stormwater Management Design Manual* [New York Department of Environmental Conservation (NYDEC) 2001].

Physical settling of the largest particles occurs in the sedimentation forebay. Physical and chemical water quality treatment occurs in the filter basin. A sand filter is commonly viewed as a system for removing mostly suspended solids. However, it has been shown that sand filters have the ability to remove dissolved phosphorus and metals (Barrett 2003; Minton 2002; Urbonas 1999). Performance of the surface sand filter used for this research is found in Roseen et al. (2006) and University of New Hampshire Stormwater Center (UNHSC 2007).

Monitoring

For this study, rainfall-runoff events were selected between August 2004 and September 2006 for a total of 17 discrete events. Automated samplers (6712SR ISCO) were used to perform the sampling program. Although the ISCO samplers collected up to 24 samplers per storm event, normally only 8–12 samples were used to characterize both influent and effluent storm-water quality. The sampling program for the system was based on analyses of various effluent hydrographs. Monitored real-time parameters included: precipitation, influent flow to the sedimentation forebay, and effluent flows from the sand filter.

Constituent analysis of water samples included: TSS, TPH-D, and zinc (Zn). Storm-water samples were analyzed by a laboratory that is state certified for drinking water and wastewater. Guidance documents on collecting environmental data and the site quality assurance project plan were followed to assure quality of the results (EPA 2002). Characteristics of the storm events selected for this research are presented in Avellaneda et al. (2009).

Model Structure

Flow Routing

Flow from the sedimentation forebay drains to the sand filter through a 25-mm orifice. Therefore, influent flows to the basin above the surface sand filter were determined by a flow routing analysis. When the forebay reaches its maximum storage capacity, flows are conveyed to the sand filter through a contracted rectangular weir ($L_w=1.57$ m). The equations and parameters used to compute effluent flows from the forebay are shown in Table 1. The storage function was determined from the forebay geometric characteristics. The effluent hydrograph was computed using a storage-indication method (Durrans et al. 2003). The method is based on a finite-difference approximation of the conservation of mass equation.

Storm-Water Treatment Model

The storm-water treatment model is a combination of a mass balance approach and a one-dimensional advection-dispersion model. A mass balance approach was implemented to determine (1) effluent concentrations from the forebay and (2) effluent concentrations from the basin above the filter media. Note that the second effluent also represents the influent concentrations to the

Table 1. Equations Used for the Storage Routing Computations

Expression	Description
$Q_o = C_{d,o} A_o (2gh_o)^{1/2}$	Orifice discharge Q_o as a function of the coefficient $C_{d,o}=0.6$, the orifice area $A_o = 5.1\times10^{-4}\ \text{m}^2$, and the effective head h_o on the orifice
$Q_w = \frac{2}{3} C_{d,w}\sqrt{2g}(L_w - 0.1Nh_w)h_w^{3/2}$	Weir discharge Q_w as a function of the coefficient $C_{d,w}$, the length of the weir crest $L_w = 1.57$ m, the number of weir end contractions $N=2$, and the effective head h_w above the weir crest
$C_{d,w} = 0.611 + 0.075(h_w/H)$	Weir discharge coefficient $C_{d,w}$ as a function of the effective head h_w above the weir crest and the height H of the weir crest above the bottom of the sedimentation basin
$S_f = A_f h + A_f h^2 + 4/3h^3$	Forebay storage volume S_f as a function of the bottom area $A_f = 7.68\ \text{m}^2$ and the water level h. Note that the water level could be the effective head on the orifice h_o or the effective head h_w above the weir crest plus H

sand filter, which are input to the transport model. The mass balance differential equation can be written as follows:

$$\frac{\partial C_{\text{out}}}{\partial t} = \frac{C_{\text{in}}Q_{\text{in}} - C_{\text{out}}Q_{\text{out}}}{S} - \frac{C_{\text{out}}}{S}\frac{\partial S}{\partial t} \tag{1}$$

Integration of Eq. (1) yields the following analytical solution:

$$C_{\text{out}}(t+1) = \frac{C_{\text{in}}Q_{\text{in}}}{Q_{\text{out}} + \frac{\partial S}{\partial t}} + \left(C_{\text{out}}(t) - \frac{C_{\text{in}}Q_{\text{in}}}{Q_{\text{out}} + \frac{\partial S}{\partial t}}\right) e^{-\left(\frac{Q_{\text{out}} + \frac{\partial S}{\partial t}}{S}\right)(t_{i+1} - t_i)} \tag{2}$$

where C_{out}=effluent concentration (ML^{-3}) at a given time; C_{in}=influent concentration (ML^{-3}); Q_{in}=influent flow rate (L^3T^{-1}); Q_{out}=effluent flow rate (L^3T^{-1}); S=storage (L^3); $\partial S/\partial t$=change in storage (L^3T^{-1}); and $t_{i+1} - t_i$=time interval. The variables of the right hand side of Eq. (2) were obtained from field data and the flow routing analysis. The effect of precipitation on the water budget was neglected since influent flow rates were much higher in magnitude. Evaporation effects were neglected since the model was only applied during storm events. Ground water effects and other infiltration sources were also not included since the system was constructed in a clay soil. Spatial variation of the variables was not considered. The final solution was obtained by systematically solving Eq. (2) for each time interval ($\Delta t = 5$ min).

A one-dimensional advection-dispersion transport model was adopted to determine effluent contaminant concentrations from the sand filter. The general equation that describes temporal and spatial variation of particle concentration within the media depth can be written as follows (Yao et al. 1971; Kretzschmar et al. 1997; Grolimund et al. 1998):

$$\frac{\partial C}{\partial t} = D\frac{\partial^2 C}{\partial z^2} - v\frac{\partial C}{\partial z} - kC \tag{3}$$

where C=concentration of suspended particles (ML^{-3}) within the filter media at (z,t); v=pore water velocity (LT^{-1}); t=time (T); z=filter media depth (L); D=hydrodynamic dispersion (L^2T^{-1}); and k=deposition rate (T^{-1}).

For this study, a forward time and central space finite difference approximation was implemented to solve Eq. (3). The method requires a grid of I points in space and N points in time. The numerical approximation of the one-dimensional transport model at the (i,n) grid point can be written as follows (Ataie-Ashtiani et al. 1996; Najafi and Hajinezhad 2008):

$$C_i^{n+1} = \left(\frac{D^*\Delta t}{\Delta z^2} + \frac{v^*\Delta t}{2\Delta z}\right)C_{i-1}^n + \left(1 - k^*\Delta t - \frac{2D^*\Delta t}{\Delta z^2}\right)C_i^n + \left(\frac{D^*\Delta t}{\Delta z^2} - \frac{v^*\Delta t}{2\Delta z}\right)C_{i+1}^n$$

$$D^* = D + \frac{\Delta t}{2}(v^2 - 2kD)$$

$$v^* = v - (\Delta t)kv$$

$$k^* = k - \frac{\Delta t}{2}k^2 \tag{4}$$

where D^*=numerical dispersion; v^*=numerical pore water velocity; and k^*=numerical deposition rate coefficient. These numerical parameters take into account the fact that the numerical discretization of Eq. (3) introduces a second-order truncation error. Ataie-Ashtiani et al. (1996) studied the numerical solution (4) and concluded that to satisfy stability criteria, the following restriction is necessary:

$$\Delta t = \frac{1}{\frac{2D^*}{\Delta z^2} + \frac{k^*}{2}} \tag{5}$$

For this study, the numerical solution of Eq. (3) required appropriate boundary conditions and some assumptions. It was assumed that the hydrodynamic dispersion and deposition rate coefficients remained constant during the runoff event. However, each runoff event was calibrated independently so that optimized parameter values were obtained on a storm by storm basis. A zero concentration value at the beginning ($t=0$) of the runoff event was used for modeling purposes. It was assumed that the effect of the accumulated mass, from previous storm events, was taking into account by allowing the deposition rate coefficient to change in between storms. The deposition rate coefficient changes as particles accumulate within the filter media. Additionally, the effect of unsaturated flow conditions was neglected. Therefore, the pore water velocity, $v = Q/(A_{\text{sf}}\phi)$, was estimated from the monitored effluent flows using a porosity $\phi=0.4$. A time interval of 15 s and a space interval of 0.07 m were sufficient to satisfy the restriction (5) in most cases; however, the model was rerun again if during the numerical solution the restriction was not met. The boundary conditions can be summarized as follows:

$$C = 0 \quad t = 0; \quad z \ge 0$$

Table 2. Summary of Samples with Concentrations Reported as BDL

Location	Format	Total number of samples	BDL samples TPH-D	Zn	TSS
Influent	Number	166	36	18	20
	Percentage	100%	23%	14%	8%
Effluent	Number	132	97	61	37
	Percentage	100%	69%	46%	21%

$$\frac{\partial C}{\partial z} = 0 \quad t \geq 0; \quad z = 0.76 \text{ m} \tag{6}$$

Objective Function

An objective function was necessary to estimate the best parameter values on a storm by storm basis. The sum-of-squares estimator was adopted and is written as follows:

$$O(\Theta) = \min \sum_{i=1}^{m} [C_{\text{obs}} - C_{\text{est}}(\Theta)]^2 \tag{7}$$

where O denotes the objective function; C_{obs} are the measured concentrations; C_{est} are the estimated concentrations (at $z = 0.76$ m) obtained from the transport model (4); Θ represents the hydrodynamic dispersion (D) and deposition rate (k) coefficients; and (m) is the number of samples taken during the runoff event.

Optimization Technique

In this study, the simulated annealing (SA) algorithm was used as the optimization technique to minimize the objective function (7). The method uses a stochastic approach to locate the parameter values that maximize or minimize the objective function. A new set of parameter values are chosen from a probability distribution that depends on the change of the objective function (ΔO) and a parameter T (Kirkpatrick et al. 1983). This probability distribution is written as follows:

$$p(\Delta O) = e^{-\frac{\Delta O}{T}} \tag{8}$$

The stochastic process is set up initially at a very high value of T so that new parameter values are highly likely to be accepted. Therefore, the parameters' space is searched extensively at the early stage of the search. The value of the parameter T is reduced during the process according to a "cooling schedule" that depends on the shape of the objective function. A solution that is not the "best" may be accepted occasionally so the algorithm does not get trapped in a local minimum.

Measured Concentrations below Detection Limit

A detection limit (DL) is reported when concentrations are below the analytical reporting limit. Such concentrations are reported as being below the analytical DL (BDL). One-half of the DL is commonly used if a discrete value is needed rather than a range (from 0 to BDL). The percentages of influent and effluent concentrations reported as BDL for each constituent are displayed in Table 2. In this study, the DLs were normally: 0.50 mg/L for TPH-D, 0.03 mg/L for Zn, and 10 mg/L for TSS. However, the reported DL could vary depending on the actual sample volume.

Estimates of the BDL concentrations can be made by implementing a probabilistic approach. In this scenario, a probability distribution is fitted to the data using only concentrations above the reported DL. Then, concentrations between zero and the DL can be drawn from the fitted probability distribution (Helsel and Hirsch 2002). Note that the accuracy of this method depends on the amount of data available above DL.

Table 3. Parameters of the Gamma Distributions Fitted to the Data

Contaminant	Total samples above DL (n)	γ ($-$)	θ (mg/L)	D_{critical} ($-$)	$D_{n,\alpha}$ ($-$)
TPH-D	35	4.61	0.15	0.23	0.13
Zn	71	2.76	0.01	0.16	0.17
TSS	95	2.12	16.67	0.14	0.07

Note: Level of significance $\alpha = 0.05$.

For this study, a gamma distribution was fitted to the data since it adequately described the measured concentrations (other distributions such as lognormal and Gumbel were tested). The parameters γ (shape) and θ (scale) of the gamma distribution were computed using the maximum likelihood estimator. The equation of the gamma distribution is written as follows:

$$p(C;\gamma,\theta) = \frac{C^{\gamma-1}e^{-\frac{C}{\theta}}}{\theta^{\gamma}\Gamma(\gamma)} \tag{9}$$

where p represents the probability of an effluent concentration C given the parameters γ and θ.

The parameter values of the fitted probability distributions are shown in Table 3. The Kolmogorov-Smirnov test (KS test) was used to assess whether or not the data followed the fitted distributions. The $D_{n,\alpha}$ statistic was computed for a level of significance $\alpha = 0.05$ (95% confidence interval) and (n) concentration values above the DL. The data follows the fitted distribution when $D_{n,\alpha} \leq D_{\text{critical}}$. Empirical and theoretical probability distributions functions (PDFs) are shown in Fig. 1. The $D_{n,\alpha}$ statistic represents the maximum vertical deviation between the empirical and theoretical data probability distributions.

Calibration Procedure

Optimal parameter values for the hydrodynamic dispersion and deposition rate coefficients were obtained on a storm by storm basis. During the optimization for a single runoff event, parameter candidates for (D) and (k) were randomly generated according to the SA algorithm. The RMS error (RMSE) was computed for each set of candidates. For the new candidates to be generated, it was necessary to establish a lower and upper limit. A range between 0 and 3×10^{-2} s^{-1} was adopted for (k) and a range between 0 and 2×10^{-3} m^2/s was adopted for (D). A linear decrement function was used to compute the parameter T of the SA algorithm. The "cooling" schedule was defined by

$$T_{j+1} = aT_j \quad j = 0, 1, \ldots, m \tag{10}$$

where T = parameter of the SA algorithm; m = number of steps of the cooling schedule; and a = reduction coefficient that varies between 0 and 1 (Hopgood 2000). For this research, these parameters were set to $T = 10{,}000$, $m = 20$, $a = 0.9$, and a total of 20,000 iterations were used. These previous parameter values were found by initially rerunning the model several times and verifying that the random walk searched the entire domain and the parameter T did not reduce too quickly. A total of 15 storms were used for calibration purposes, and two storms were selected for model validation.

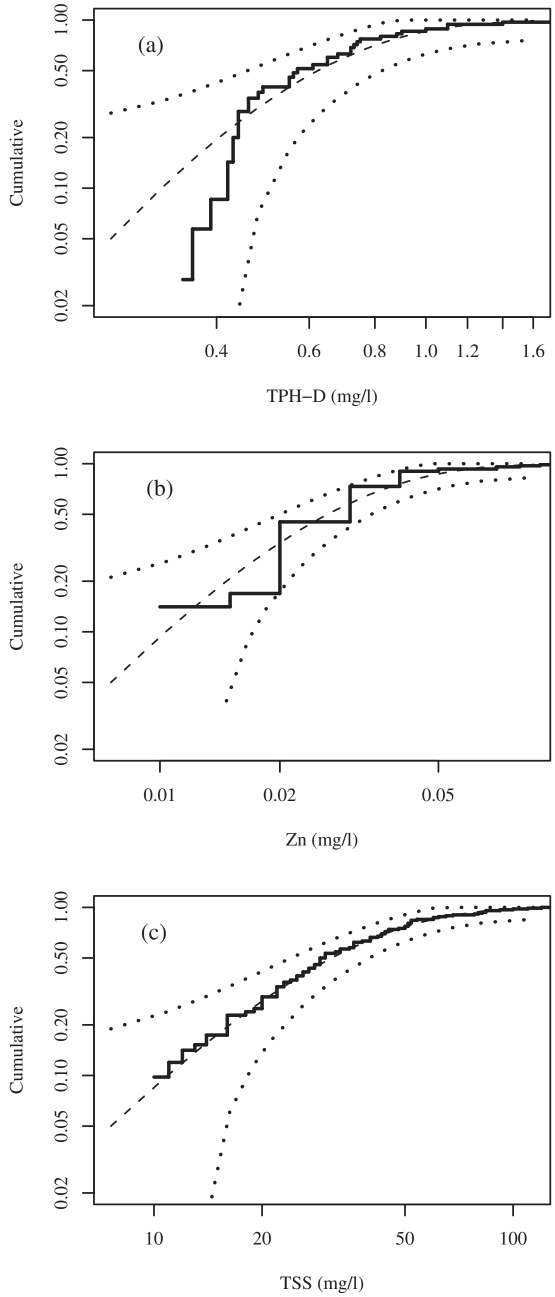

Fig. 1. Empirical (solid line) and theoretical (dashed line) data probability distributions. A 95% confidence interval is reported (dotted line).

Results

Model Application

Model results for some of the rainfall-runoff events considered in this study are shown in Figs. 2 and 3. Influent and effluent monitored hydrographs are also plotted. Influent pollutographs for all the constituents of study were obtained from a calibrated accumulation and wash-off model (Avellaneda et al. 2009). Estimated concentrations are plotted along with the observed concentration values. RMSE values are also reported.

The influent hydrograph for the March 8, 2005 event increased gradually, reached a maximum peak flow, and then decayed [Fig. 2(a)]. A delay was clearly observed in the effluent hydrograph. This is due to the sand filter's storage capacity and infiltration rate; although, it also depends on factors such as rainfall duration and intensity. An influent peak flow reduction was also observed. For all the constituents, the first observed effluent concentration was reported as BDL. The model does not explain the reported BDL concentration of the first sample for TSS and Zn, and results tend to follow the trend of the subsequent higher concentrations. A below DL concentration in the early part of the storm was in general unusual. Normally, concentrations below DL were reported toward the end of the storm.

Model results for the April 20, 2005 rainfall-runoff event are shown in Fig. 3. Multiple flow peaks were observed on the influent hydrograph [Fig. 3(a)]. As expected, the influent hydrograph is attenuated by the storage available in this storm-water system, producing a smooth effluent hydrograph. The last three concentration values were reported below the DL for Zn, the last one for TSS, and only the first two sample concentrations were reported above the DL for TPH-D. The model described the general trend observed of the measured concentrations.

The optimized parameter values for all the rainfall-runoff events and constituents included in this study are presented in Table 4. RMSE values are reported. Box plots for the optimized parameter values are shown in Fig. 4. The median deposition rate coefficient was $6.9 \times 10^{-4}\ \mathrm{s}^{-1}$ for TPH-D, $3.1 \times 10^{-4}\ \mathrm{s}^{-1}$ for TSS, and $3.8 \times 10^{-3}\ \mathrm{s}^{-1}$ for Zn. The median hydrodynamic dispersion coefficient was $1.9 \times 10^{-4}\ \mathrm{m}^2/\mathrm{s}$ for TPH-D, $2.7 \times 10^{-4}\ \mathrm{m}^2/\mathrm{s}$ for TSS, and $1.1 \times 10^{-3}\ \mathrm{m}^2/\mathrm{s}$ for Zn. Different probability distributions were fitted to the optimized parameter values and tested. It was found that the gamma distribution was appropriate to represent the CDFs obtained from the optimized values. The parameters of the gamma distribution fitted to the data are shown in Table 5.

Event Mean Concentration (EMC)

An EMC is a parameter commonly used to characterize contaminant concentrations of a storm event (Sansalone and Chad 2004; Lee and Bang 2000). The EMC of a storm event is defined as the total contaminant load divided by the total runoff volume. When discrete samples are collected during the duration of the storm, Eq. (11) can be used to compute the EMC

$$\mathrm{EMC} = \frac{\sum_{i=1}^{m} Q_i C_i \Delta t_i}{\sum_{i=1}^{m} Q_i \Delta t_i} \tag{11}$$

where EMC=EMC (ML^{-3}); Q_i and C_i=average flows (L^3T^{-1}) and concentrations (ML^{-3}) within the time interval Δt_i (T); and m =total number of time intervals. EMCs have also been used to evaluate the performance of storm-water treatment measures (Barret 2003, 2005; Roseen et al. 2006). In this study, EMCs were computed for the storms considered for calibration. Cumulative distribution functions (CDFs) for the observed and estimated effluent EMCs are shown in Fig. 5. Estimated effluent EMCs were computed using the estimated pollutographs obtained after calibration and the respective effluent hydrograph. The KS test was performed to assess whether or not the estimated effluent CDF followed the distribution of the observed effluent CDF. The estimated effluent CDF for TPH-D did not pass the KS test since $D_{n,\alpha} > D_{\text{critical}}$ for a level of significance $\alpha=0.05$ ($D_{n,\alpha}=0.46$, $D_{\text{critical}}=0.39$, $n=11$ storms). The statistical results suggest that the model is overestimating effluent EMCs for TPH-D. For TSS

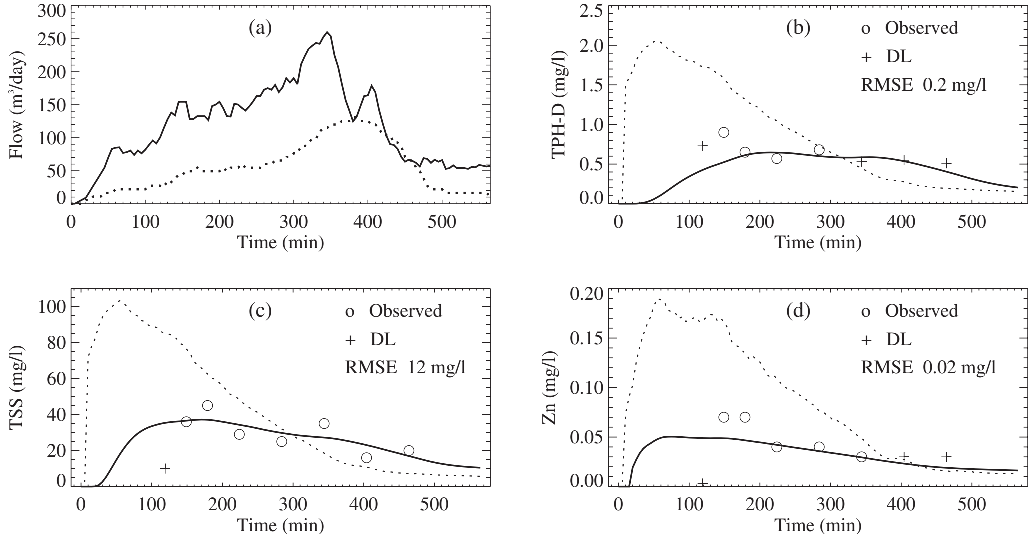

Fig. 2. Results for the March 8, 2005 rainfall-runoff event. Influent (solid line) and effluent (dashed line) flows are shown in (a). Influent (dashed line) and calibrated (solid line) effluent concentrations are shown in (b)–(d). Observed effluent concentrations and DL are plotted as discrete points. The RMSE is reported. Optimized parameter values are shown in Table 4.

and Zn, the estimated effluent CDFs passed the KS test, which suggests that the calibrated model preserved the distribution of the observed effluent EMCs.

Monte Carlo Simulation

A single set of parameter values should not be used for modeling purposes. As it has been reported so far in this study, optimized model parameter values vary among rainfall-runoff events. One could determine the PDF of the model parameters when data are available. When the parameters' PDFs are provided, then a Monte Carlo simulation can be performed to assess the predicting capabilities of the model. Monte Carlo simulations incorporate uncertainty into the analysis and it has been recommended as a useful tool when assessing the water quality characteristics that would result from different environmental scenarios (Beck 1987; Walker 1994).

Simulation results for the May 2, 2006 and May 9, 2006 rainfall-runoff events are shown in Fig. 6 and Fig. 7, respectively. For this study, the estimates of the 10th, 30th, 70th, and 90th percentiles of the predictions were used to define the uncertainty limits. The dashed line represents the influent concentrations and the central solid line indicates the expected effluent concentrations. The dark shaded region indicates the 30 and 70% uncertainty limits. The light gray shaded region indicates the 10 and 90% uncertainty limits. Observed concentration values and the reported DLs were plotted as discrete points. The number of

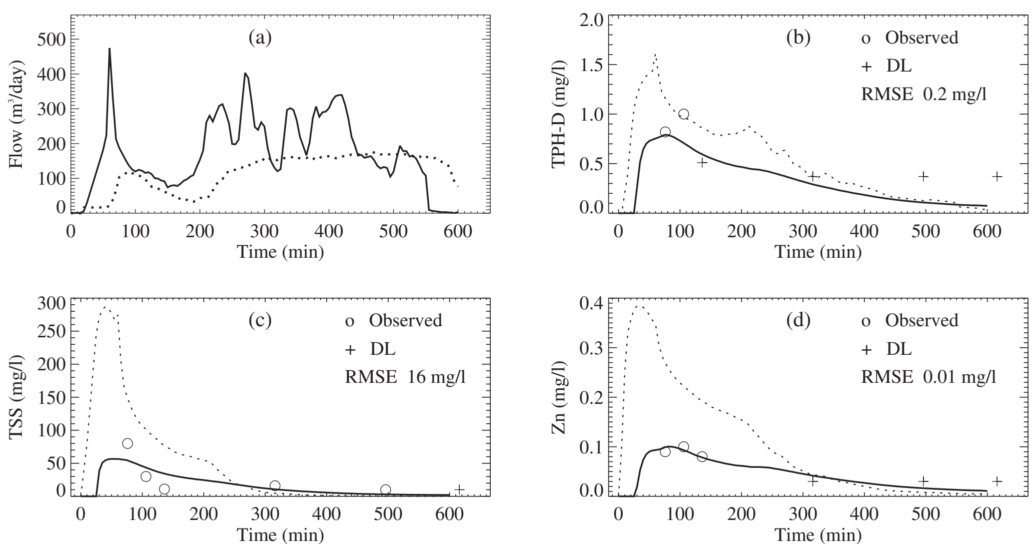

Fig. 3. Results for the April 20, 2005 rainfall-runoff event. Influent (solid line) and effluent (dashed line) flows are shown in (a). Influent (dashed line) and calibrated (solid line) effluent concentrations are shown in (b)–(d). Observed effluent concentrations and DL are plotted as discrete points. The RMSE is reported. Optimized parameter values are shown in Table 4.

Table 4. Optimized Model Parameters Values

Rainfall- runoff event	TPH-D k [s^{-1}] ($\times10^{-5}$)	TPH-D D [m^2/s] ($\times10^{-5}$)	TPH-D RMSE (mg/L)	TSS k [s^{-1}] ($\times10^{-5}$)	TSS D [m^2/s] ($\times10^{-5}$)	TSS RMSE (mg/L)	Zn k [s^{-1}] ($\times10^{-5}$)	Zn D [m^2/s] ($\times10^{-5}$)	Zn RMSE (mg/L)
September 18, 2004	1,300	114	0.13	2	19	48	1,071	112	0.013
October 30, 2004	734	114	0.04	4	2	12	201	112	0.011
January 14, 2005	NA	NA	NA	30	6	9	NA	NA	NA
February 10, 2005	17	19	0.12	NA	NA	NA	48	8	0.010
March 8, 2005	22	1	0.20	33	4	12	1,155	116	0.017
March 28, 2005	3	17	0.31	11	2	42	381	112	0.012
April 20, 2005	241	25	0.20	673	48	16	185	16	0.011
August 13, 2005	39	11	0.32	982	114	11	NA	NA	NA
September 15, 2005	14	1	0.14	1	31	32	1,281	115	0.003
November 6, 2005	NA	NA	NA	NA	NA	NA	511	111	0.003
November 30, 2005	69	9	0.14	NA	NA	NA	1,012	114	0.003
December 16, 2005	NA	NA	NA	88	24	3	99	11	0.005
January 11, 2006	462	115	0.30	0.4	89	31	7	106	0.010
February 17, 2006	235	112	0.24	1,149	112	8	761	73	0.003
March 13, 2006	NA	NA	NA	502	106	9	147	16	0.002

Note: "NA" indicates that data are not available.

simulations was set to 5,000 for each constituent. The fitted gamma distributions (Table 5) were used to generate values for the hydrodynamic dispersion and deposition rate coefficients.

Results of the Monte Carlo simulation indicate an acceptable performance of the model since, in general, observed concentration fell within the uncertainty limits. For the May 2, 2006 rainfall-runoff event, four observed TSS concentrations were reported below the DL (10 mg/L). The model was able to predict TSS concentrations for the first (263 min) and third (293 min) samples. However, TSS concentrations for the sixth (473 min) and eighth (653 min) samples fell outside the uncertainty limits. The model did predict effluent TSS concentrations less or equal to the analytical DL. For TPH-D and Zn, all observed concentrations but the first one were reported below the DL. The DL was approximately 0.40 mg/L for TPH-D and 0.01 mg/L for Zn. The model did predict effluent TPH-D and Zn concentrations below the DL [Figs. 6(a and b)].

Monte Carlo simulation results for the May 9, 2006 rainfall-runoff event are shown in Fig. 7. For this event, all observed TPH-D effluent concentrations were reported below the DL [Fig. 7(a)]. Although the model did predict concentrations BDL for TPH-D, concentrations for the first two samples were overestimated. Few concentrations were reported above the DL for TSS and Zn. The DL was approximately 10 mg/L for TSS and 0.01 mg/L for Zn. The model was capable of predicting the first two samples for both TSS [Fig. 7(c)] and Zn [Fig. 7(b)] within the 90% uncertainty limit. One observed TSS concentration (430 min) fell outside the uncertainty limits. For these two constituents, simulation results predicted concentrations values below the DL. Note that results of the validation phase would have been more robust if lower DLs had been selected for the collected samples.

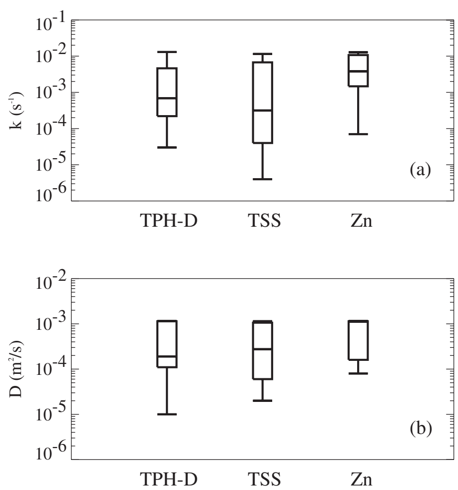

Fig. 4. Box plot of optimized model parameter values

Table 5. Parameters of the Gamma Distributions Fitted to the Optimized Parameter Values

Parameter	Contaminant	Total number of storms (n)	γ ($-$)	θ (mg/L)	$D_{critical}$ ($-$)	$D_{n,\alpha}$ ($-$)
k	TPH-D	11	0.49	0.0059	0.39	0.16
	Zn	13	1.27	0.0041	0.36	0.20
	TSS	12	0.46	0.0063	0.38	0.30
D	TPH-D	11	0.89	0.0006	0.39	0.26
	Zn	13	2.79	0.0003	0.36	0.38
	TSS	12	1.03	0.0005	0.38	0.22

Note: Level of significance $\alpha=0.05$.

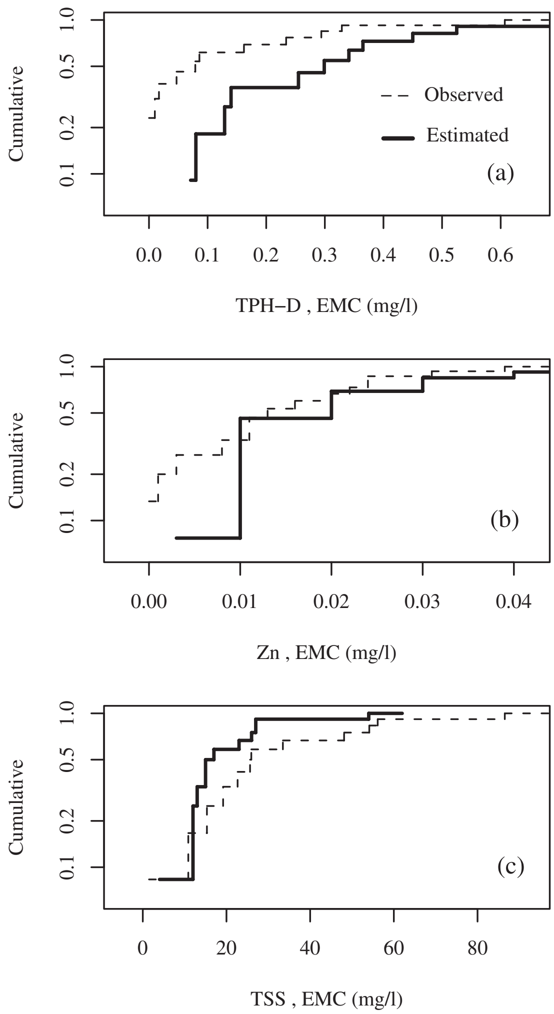

Fig. 5. Sand filter CDF of EMCs: observed (dashed line) and estimated (solid line)

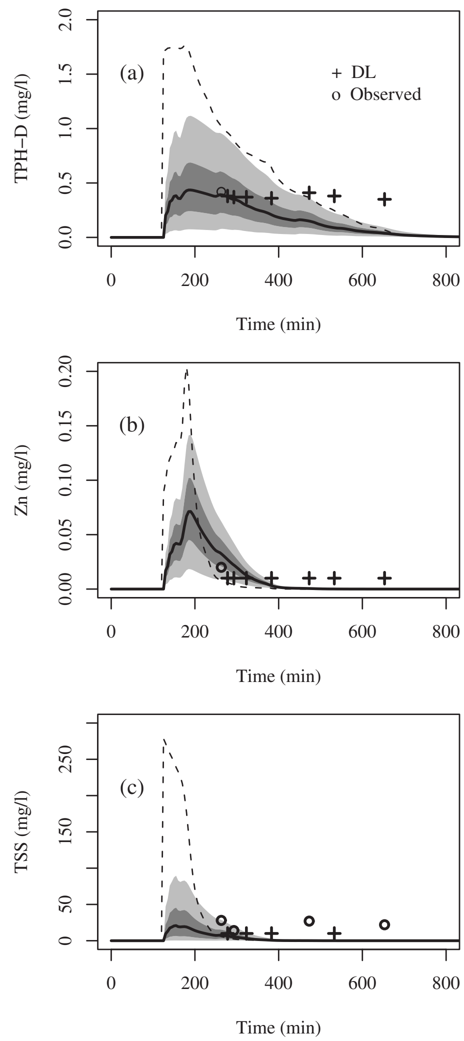

Fig. 6. Monte Carlo simulations of predicted effluent concentrations for the May 2, 2006 rainfall-runoff event. Uncertainty limits are reported as percentiles of the predicted values. The dark shaded region indicates the 30 and 70% uncertainty limits. The light gray shaded region indicates the 10 and 90% uncertainty limits. Observed concentrations values and the reported DLs are plotted as discrete values. The influent pollutograph (dashed line) and the expected effluent pollutograph (solid line) are reported.

Conclusions

This study examined the predicting capabilities of a storm-water treatment model for estimating effluent contaminant concentrations from a surface sand filter. The model was based on a mass balance approach and a one-dimensional advection-dispersion transport model. Two parameters, the deposition rate and the hydrodynamic dispersion coefficients, represented the combined effects of various removal and transport mechanisms. Field data consisted of influent and effluent flows to the system, and observed concentrations for three constituents. The surface sand filter was monitored for storm-water quality at a parking lot in Durham.

Seventeen rainfall-runoff events were monitored from 2004 to 2006. Fifteen of those events were selected for calibration and the remaining two were left for validation. Optimized deposition rate and dispersion coefficients were provided for TSS, TPH-D, and Zn on a storm by storm basis. The median deposition rate coefficient was $6.9 \times 10^{-4}\ \text{s}^{-1}$ for TPH-D, $3.1 \times 10^{-4}\ \text{s}^{-1}$ for TSS, and $3.8 \times 10^{-3}\ \text{s}^{-1}$ for Zn. The median hydrodynamic dispersion coefficient was $1.9 \times 10^{-4}\ \text{m}^2/\text{s}$ for TPH-D, $2.7 \times 10^{-4}\ \text{m}^2/\text{s}$ for TSS, and $1.1 \times 10^{-3}\ \text{m}^2/\text{s}$ for Zn. A gamma distribution seemed to describe the variability of the optimized parameter values. For the runoff events selected for calibration, the model seemed to be able to preserve the overall distribution of the observed effluent EMCs for TSS and Zn; however, it overestimated the distribution of the EMCs for TPH-D.

The validation phase consisted of a Monte Carlo simulation to assess water quality performance of the treatment model using two runoff events. Parameter values were drawn from the gamma distributions fitted to the optimized values. Uncertainty limits were defined as the 10th and 90th percentile of the predictions. Results of the validation phase show an acceptable performance of the model since, in general, estimated effluent concentrations fell within the uncertainty limits. However, results of the validation phase would have been more robust if lower DLs had been selected for the collected samples.

The statistical results provided in this study could be used in more complex models such as Bayesian applications. Additionally, one could add more complexity to the treatment model by incorporating other parameters that account for spatial variation and other removal mechanisms within the system. Further re-

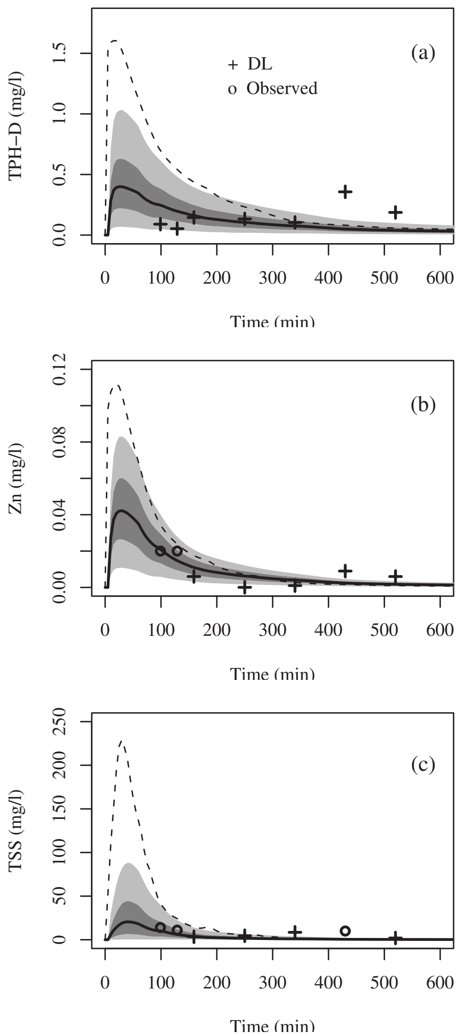

Fig. 7. Monte Carlo simulations of predicted effluent concentrations for the May 9, 2006 rainfall-runoff event. Uncertainty limits are reported as percentiles of the predicted values. The dark shaded region indicates the 30 and 70% uncertainty limits. The light gray shaded region indicates the 10 and 90% uncertainty limits. Observed concentrations values and the reported DLs are plotted as discrete values. The influent pollutograph (dashed line) and the expected effluent pollutograph (solid line) are reported.

search should explore the relationship between the deposition rate coefficient and the volumetric specific deposit, defined as the volume of deposited particles per unit filter bed volume. A more complex physical approach could incorporate the effect of pore water velocity on the dispersion and deposition rate coefficients. In addition, the calibration approach can be improved by using the measured influent concentrations directly rather than an estimate of the pollutograph generated by an accumulation and wash-off model (calibrated using the measured concentrations). An alternative approach may be to calibrate simultaneously the accumulation and wash-off model and the sand filter transport equations.

Acknowledgments

The UNH Stormwater Center is housed within the Environmental Research Group (ERG) at the University of New Hampshire (UNH) in Durham, New Hampshire. Funding for the program was and continues to be provided by the Cooperative Institute for Coastal and Estuarine Environmental Technology (CICEET) and the National Oceanic and Atmospheric Administration (NOAA). The writers acknowledge the significant contributions made by anonymous reviewers.

References

Ataie-Ashtiani, B., Lockington, D. A., and Volker, R. E. (1996). “Numerical correction for finite-difference solution of advection-dispersion equation with reaction.” *J. Contam. Hydrol.*, 23(1–2), 149–156.

Avellaneda, P., Ballestero, T., Roseen, R., and Houle, J. (2009). “On parameter estimation of an urban stormwater runoff model.” *J. Environ. Eng.*, 135(8), 595–608.

Barrett, M. (2003). “Performance, cost, and maintenance requirements of Austin sand filters.” *J. Water Resour. Plann. Manage.*, 129(3), 234–242.

Barrett, M. (2005). “Performance comparison of structural stormwater best management practices.” *Water Environ. Res.*, 77(1), 78–86.

Beck, M. B. (1987). “Water quality modeling: A review of the analysis of uncertainty.” *Water Resour. Res.*, 23(8), 1393–1442.

Boyd, R. H., and Ghosh, M. M. (1974). “An investigation of the influences of some physicochemical variables on porous-media filtration.” *J. Am. Water Works Assoc.*, 66(2), 94–98.

Campos, L., Smith, S. R., and Graham, N. J. (2006a). “Deterministic-based model of slow sand filtration. I: Model development.” *J. Environ. Eng.*, 132(8), 872–886.

Campos, L., Smith, S. R., and Graham, N. J. (2006b). “Deterministic-based model of slow sand filtration. II: Model application.” *J. Environ. Eng.*, 132(8), 887–894.

Durrans, S. R., Dietrich, K., Ahmad, M., Barnard, T. E., Hjorth, P., and Pitt, R. (2003). *Stormwater conveyance modeling and design*, Heastad, Waterbury, Conn.

EPA. (1996). “Overview of the stormwater program.” *Rep. No. EPA 833-R-96-008*, Office of Water, U.S. EPA, Washington, D.C.

EPA. (1999). “Stormwater technology fact sheet: Sand filters.” *Rep. No. EPA 832-F-99-007*, U.S. EPA, Washington, D.C.

EPA. (2002). “Urban stormwater BMP performance monitoring.” *Rep. No. EPA-821-B-02-001*, Office of Water, U.S. EPA, Washington, D.C.

Grolimund, D., Elimelech, M., Borkovec, M., Barmettler, K., Kretzschmar, R., and Sticher, H. (1998). “Transport of in situ mobilized colloidal particles in packed soil columns.” *Environ. Sci. Technol.*, 32(22), 3562–3569.

Helsel, D. R., and Hirsch, R. M. (2002). “Statistical methods in water resources.” *Technical Rep.*, USGS.

Hopgood, A. A. (2000). *Intelligent systems for engineers and scientists*, 2nd Ed., CRC, Boca Raton, Fla.

Iwasaki, T. (1937). “Some notes on sand filtration.” *J. Am. Water Works Assoc.*, 29(10), 1591–1602.

Keblin, M. V., Barrett, M. E., Malina, J. F., and Charbeneau, R. J. (1997). “The effectiveness of permanent highway runoff controls: Sedimentation/infiltration systems.” *Research Rep. No. 97–4*, Center for Research in Water Resources, Univ. of Texas at Austin, Austin, Tex., ⟨http://www.crwr.utexas.edu/reports/pdf/1997/rpt97-4.pdf⟩ (June 1, 2009).

Kirkpatrick, S., Gelatt, C. D. Jr., and Vecchi, M. P. (1983). “Optimization by simulated annealing.” *Science*, 220(4598), 671–680.

Kretzschmar, R., Barmettler, K., Grolimund, D., Yan, Y., Borkovec, M., and Sticher, H. (1997). “Experimental determination of colloid deposition rates and collision efficiencies in natural porous media.” *Water Resour. Res.*, 33(5), 1129–1137.

Lee, J. H., and Bang, W. (2000). “Characterization of urban stormwater runoff.” *Water Res.*, 34(6), 1773–1780.

Li, H., and Davis, A. P. (2008a). "Urban particle capture in bioretention media. I: Laboratory and field studies." *J. Environ. Eng.*, 134(6), 409–418.
Li, H., and Davis, A. P. (2008b). "Urban particle capture in bioretention media. II: Theory and model development." *J. Environ. Eng.*, 134(6), 419–432.
Mays, D. C., and Hunt, J. R. (2005). "Hydrodynamic aspects of particle clogging in porous media." *Environ. Sci. Technol.*, 39(2), 577–584.
Minton, G. (2002). *Stormwater treatment: Biological, chemical, and engineering principles*, Resource Planning Associates, Seattle, Wash.
Najafi, H. S., and Hajinezhad, H. (2008). "Solving one-dimensional advection-dispersion with reaction using some finite difference methods." *Appl. Math. Sci.*, 2(53), 2611–2618.
New York Dept. of Environmental Conservation (NYDEC). (2001). *New York State stormwater management design manual*, Center for Watershed Protection, Ellicott City, Md.
Roseen, R. M., Ballestero, T. P., Houle, J. H., Avellaneda, P. M., Wildey, R., and Briggs, J. (2006). "Storm water low-impact development, conventional structural, and manufactured treatment strategies for parking lot runoff." *Journal of the Transportation Research Board*, 1984, 135–147.
Sansalone, J., and Chad, M. C. (2004). "First flush concepts for suspended and dissolved solids in small impervious watersheds." *J. Environ. Eng.*, 130(11), 1301–1314.
Tufenkji, N., and Elimelech, M. (2004). "Correlation equation for predicting single-collector efficiency in physicochemical filtration in saturated porous media." *Environ. Sci. Technol.*, 38(2), 539–536.
Univ. of New Hampshire Stormwater Center (UNHSC). (2007). "Univ. of New Hampshire Stormwater Center: 2007 annual report." ⟨http://www.unh.edu/erg/cstev/2007_stormwater_annual_report.pdf⟩ (June 1, 2009).
Urbonas, B. R. (1999). "Design of a sand filter for stormwater quality enhancement." *Water Environ. Res.*, 71(1), 102–113.
Walker, J. F. (1994). "Statistical techniques for assessing water-quality effects of BMPs." *J. Irrig. Drain. Eng.*, 120(2), 334–347.
Yao, K., Habibian, M. T., and O'Melia, C. R. (1971). "Water and waste water filtration. Concepts and applications." *Environ. Sci. Technol.*, 5(11), 1105–1112.